Article

Lipophilic G-Quadruplexes Are Self-Assembled Ion Pair Receptors, and the Bound Anion Modulates the Kinetic Stability of These Complexes

Xiaodong Shi, Katherine M. Mullaugh, James C. Fettinger,
Yun Jiang, Steven A. Hofstadler, and Jeffery T. Davis

J. Am. Chem. Soc., **2003**, 125 (36), 10830-10841• DOI: 10.1021/ja035267n • Publication Date (Web): 16 August 2003

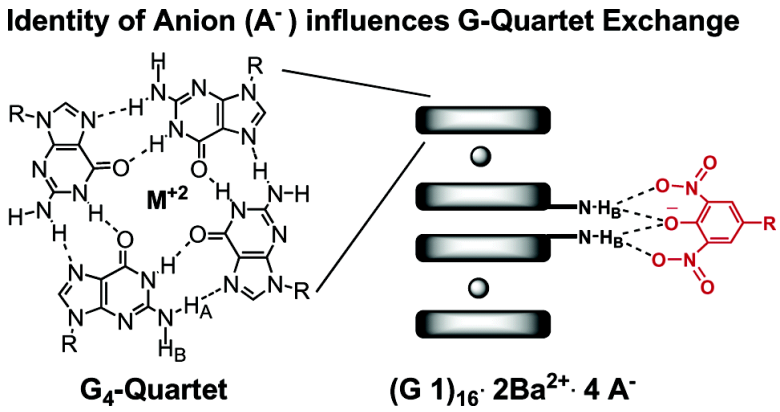

More About This Article

Additional resources and features associated with this article are available within the HTML version:

- Supporting Information
- Links to the 5 articles that cite this article, as of the time of this article download
- Access to high resolution figures
- Links to articles and content related to this article
- Copyright permission to reproduce figures and/or text from this article

View the Full Text HTML

J|A|C|S
ARTICLES
Published on Web 08/16/2003

Lipophilic G-Quadruplexes Are Self-Assembled Ion Pair Receptors, and the Bound Anion Modulates the Kinetic Stability of These Complexes

Xiaodong Shi,[†] Katherine M. Mullaugh,[†] James C. Fettinger,[†] Yun Jiang,[‡] Steven A. Hofstadler,[‡] and Jeffery T. Davis*,[†]

Contribution from the Department of Chemistry and Biochemistry, University of Maryland, College Park, Maryland 20742, and Ibis Therapeutics, 2292 Faraday Avenue, Carlsbad, California 92008

Received March 21, 2003; E-mail: jd140@umail.umd.edu

Abstract: With an eye toward the eventual selective modification of noncovalent structures, we used ESI-MS, X-ray crystallography, and NMR spectroscopy to study the anion's influence on the structure and dynamics of self-assembled ion pair receptors formed from guanosine G **1**. We compared five complexes of formula (G **1**)$_{16}$·2Ba^{2+}·4A^{-} containing different organic anions: 2,4,6-trinitrophenolate (**2**), 2,6-dinitrophenolate (**3**), 4-methyl-2,6-dinitrophenolate (**4**), 4-methoxy-2,6-dinitrophenolate (**5**), and 2,5-dinitrophenolate (**6**). Crystallography reveals that anion−nucleobase hydrogen bond geometry is sensitive to both phenolate basicity and structure. For the 2,6-substituted anions **2**−**5**, progressive shortening of anion−nucleobase hydrogen bonds is correlated with increased phenolate basicity. Lipophilic G-quadruplexes with different anions also have much different kinetic stabilities in CD_2Cl_2 solution. Proton NMR shows that free **6** exchanges faster with G-quadruplex-bound anion than do the 2,6-dinitrophenolates **2**−**5**. The increased lability of **6** is probably because, unlike the 2,6-dinitrophenolates, this anion cannot effectively chelate separate G_8·M^{2+} octamers via anion−nucleobase hydrogen bonds. In addition to these structural effects, the anion's basicity modulates the anion exchange rate between its free and bound states. 2D EXSY NMR shows that **3** and **5** exchange about 7 times slower than the less basic picrate (**2**). The use of **3**, a relatively basic dinitrophenolate that hydrogen bonds with the amino groups of the two "inner" G_4-quartets, resulted in extraordinary kinetic stabilization of the G-quadruplex in CD_2Cl_2. Thus, no isomerization product (G **1**)$_8$·Ba^{2+}·(G **1**)$_8$·Sr^{2+}·4(**3**) was observed even 2 months after the separate G-quadruplexes (G **1**)$_{16}$·2Ba^{2+}·4(**3**) and (G **1**)$_{16}$·2Sr^{2+}·4(**3**) were combined in CD_2Cl_2. In sharp contrast, G-quadruplexes containing the isomeric **6** anion have isomerization half-lives of approximately $t_{1/2} = 30$ min under identical conditions. All the evidence indicates that the structure and electronics of the organic anions, bound to the assembly's periphery, are crucial for controlling the kinetic stability of these cation-filled G-quadruplexes.

Introduction

Noncovalent synthesis often relies on self-assembly of multiple components into discrete supramolecules.[1] Self-assembly's major advantage is that it operates under thermodynamic control. With the right building blocks, large structures can be made rapidly, inexpensively, and in high yield.[2,3] While a hydrogen-bonded assembly may well be thermodynamically stable, its parts are in flux, breaking off and adding back to the assembly. Depending on the system and conditions, component exchange takes somewhere between milliseconds and months, with shorter time scales being the norm for hydrogen-bonded assemblies. As nanotechnology begins to require defined structures and devices that are 1−1000 nm in size, there will undoubtedly be many occasions that require strategies for kinetically stabilizing supramolecular assemblies. For example, if you want to modify a particular region of a noncovalent assembly, you need to be sure that the components stay in place during, and after, the synthetic operation. Relative to systems

* To whom correspondence should be addressed.
[†] University of Maryland.
[‡] Ibis Therapeutics.

(1) (a) Whitesides, G. M.; Simanek, E. E.; Mathias, J. P.; Seto, C. T.; Chin, D. N.; Mammen, M.; Gordon, D. M. *Acc. Chem. Res.* **1995**, *28*, 37−44. (b) Prins, L. J.; Reinhoudt, D. N. Timmerman, P. *Angew. Chem., Int. Ed.* **2001**, *40*, 2383−2426. (c) Reinhoudt D. N.; Crego-Calama, M. *Science* **2002**, *295*, 2403−2407. (d) Stoddart, J. F.; Tseng, H. *Proc. Natl. Acad. Sci. U.S.A.* **2002**, *99*, 4797−4800.

(2) Selected reviews that focus on hydrogen-bonded mediated self-assembly: (a) Lindsey, J. S. *New J. Chem.* **1991**, *15*, 153−180. (b) Lawrence, D. S.; Jiang, T.; Levett, M. *Chem. Rev.* **1995**, *95*, 2229−2260. (c) Zimmerman, S. C.; Corbin, P. S. *Struct. Bonding* **2000**, *96*, 63−94. (d) Kato, T. *Struct. Bonding* **2000**, *96*, 95−146. (e) Brunsveld, L.; Folmer, B. J. B.; Meijer, E. W.; Sijbesma, R. P. *Chem. Rev.* **2001**, *101*, 4071−4097.

(3) For selected recent examples of hydrogen-bonded assemblies see: (a) Zimmerman, S. C.; Zeng, F.; Reichert, D. E.; Kolotuchin, S. V. *Science* **1996**, *271*, 1095−1098. (b) Prins, L. J.; Huskens, J.; De Jong, F.; Timmerman, P.; Reinhoudt, D. N. *Nature* **1999**, *398*, 498−502. (c) Cai, M.; Marlow, A. L.; Fettinger, J. C.; Fabris, D.; Haverlock, T. J.; Moyer, B. A.; Davis, J. T. *Angew. Chem., Int. Ed.* **2000**, *39*, 1283−1285. (d) Fenniri, H.; Mathivanan, P.; Vidale, K. L.; Sherman, D. M.; Hallenga, K.; Wood, K. V.; Stowell, J. G. *J. Am. Chem. Soc.* **2001**, *123*, 3854−3855. (e) Carrasco, H.; Foces-Foces, C.; Perez, C.; Rodriguez, M. L.; Martin, J. D. *J. Am. Chem. Soc.* **2001**, *123*, 11970−11981. (f) Brunsveld, L.; Meijer, E. W.; Prince, R. B.; Moore, J. S. *J. Am. Chem. Soc.* **2001**, *123*, 7978−7984. (g) Ma, Y.; Kolotuchin, S. V.; Zimmerman, S. C. *J. Am. Chem. Soc.* **2002**, *124*, 13757−13769. (h) Fenniri, H.; Deng, B.-L.; Ribbe, A. E *J. Am. Chem. Soc.* **2002**, *124*, 11064−11072.

10.1021/ja035267n CCC: $25.00

held together by reversible covalent bonds,[4] by metal ion coordination bonds,[5] or by mechanically locked bonds,[6] hydrogen-bonded assemblies that are kinetically stable are fewer. Hydrogen-bonded capsules can be stabilized by guest inclusion.[7] Guest inclusion strengthens the hydrogen bonds that hold the capsule together and influences component exchange rates. The capsules' kinetic stability can also be increased by structural modifications. Böhmer showed that mechanical entanglement of calixarene subunits slows ligand and guest exchange.[8] Another effective method to lock a hydrogen-bonded assembly is to covalently modify the complex after formation.[9] Hydrogen-bonded complexes can also be kinetically stabilized by increasing the number of hydrogen bonds that hold the assembly together. Reinhoudt and colleagues showed this with calixarene rosettes; the exchange half-life for a hydrogen-bonded melamine increased from 8 min in a double rosette to 155 h in a hexarosette.[10] Chiral rosettes also have high racemization barriers, because the process requires so many hydrogen bonds to be broken.[11] A less common approach toward stabilizing hydrogen-bonded assemblies is to use components that interact with functional groups on the assembly's exterior.[12,13] This last approach is taken in this study.

In this paper, we show how to control some dynamic properties of a class of self-assembled ionophores that recognize ion pairs. We show that organic anions that hydrogen bond to the assembly's exterior influence the assembly's kinetic stability. These anions bridge individual components, much like clips holding pieces of material together. Varying the anions' H-bond geometry or H-bond strength modulates the exchange of assembly components. The anion's influence can be quite significant; a supramolecular isomerization that is complete within minutes when 2,5-dinitrophenolate is the anion does not occur if an isomeric 2,6-dinitrophenolate is used as the anion.

As cation and anion recognition has become better understood,[14,15] attention has turned toward ion pair recognition. One approach for ion pair recognition is to use dual receptors consisting of one ionophore for the cation and one for the anion.[16] Another strategy is to build a "heteroditopic" receptor by grafting two hosts into a single compound. A ditopic receptor has a Lewis basic site for cation coordination, and a Lewis or Brönsted acid for anion binding.[17,18] Ditopic receptors are often allosteric, and coordination of one ion influences binding of the partner ion.[19,20] Instead of using covalent ionophores with separate binding sites, self-assembly of a ditopic receptor from multiple components is an attractive strategy for ion pair recognition.[12,21−23] Lipophilic nucleosides, such as 5′-*tert*-butyldimethylsilyl-2′,3′-isopropylideneguanosine (G **1**), form cation-templated hydrogen-bonded G-quartets in organic solvents,[24,25] similar to the structures formed by guanosine mononucleotides and oligonucleotides in water.[26]

As depicted in Figure 1, the hexadecameric G-quadruplex can be described by three levels of organization. This figure, which describes the structure $(G\ \mathbf{1})_{16}\cdot 3K^+/1Cs^+\cdot 4Pic^-$ ($Pic^- =$ picrate),[24a] is meant to be a schematic and does not imply a specific assembly mechanism. Four molecules of G **1** form a

(4) Rowan, S. J.; Cantrill, S. J.; Cousins, G. R. L.; Sanders, J. K. M.; Stoddart, J. F. *Angew. Chem., Int. Ed.* **2002**, *41*, 898−952.

(5) (a) Fujita, M.; Ibukuro, F.; Yamaguchi, K.; Ogura, K. *J. Am. Chem. Soc.* **1995**, *117*, 4175−4176. (b) Kuehl, C. J.; Huang, S. D.; Stang, P. J. *J. Am. Chem. Soc.* **2001**, *123*, 9634−9641. (c) Terpin, A. J.; Ziegler, M.; Johnson, D. W.; Raymond, K. N. *Angew. Chem., Int. Ed.* **2001**, *40*, 157−160. (d) Fochi, F.; Jacopozzi, P.; Wegelius, E.; Rissanen, K.; Cozzini, P.; Marastoni, E.; Fisicaro, E.; Manini, P.; Fokkens, R.; Dalcanale, E. *J. Am. Chem. Soc.* **2001**, *123*, 7539−7552.

(6) (a) Asakawa, M.; Ashton, P. R.; Ballardini, R.; Balzani, V.; Belohradsky, M.; Gandolfi, T.; Kocian, O.; Prodi, L.; Raymo, F. M.; Stoddart, J. F.; Venturi, M. *J. Am. Chem. Soc.* **1997**, *119*, 302−310. (b) Ashton, P. R.; Baxter, I.; Fyfe, M. C. R.; Raymo, F. M.; Spencer, N.; Stoddart, J. F.; White, A. J. P.; Williams, D. J. *J. Am. Chem. Soc.* **1998**, *120*, 2297−2307. (c) Chang, S.-Y.; Jang, H.-Y.; Jeong, K.-S. *Chem.−Eur. J.* **2003**, *9*, 1535−1541.

(7) (a) Hof, F.; Nuckolls, C.; Craig, S. L.; Mart1n, T.; Rebek, J. *J. Am. Chem. Soc.* **2000**, *122*, 10991−10996. (b) Hof, F.; Nuckolls, C.; Craig, S. L.; Mart1n, T.; Rebek, J. *J. Am. Chem. Soc.* **2000**, *122*, 4251−4252. (c) Vysotsky, M. O.; Böhmer, V. *Org. Lett.* **2000**, *2*, 3571−3574. (d) Cai, M.; Sidorov, V.; Lam, Y. F.; Flowers, R. A.; Davis, J. T. *Org. Lett.* **2000**, *2*, 1665−1668.

(8) (a) Vysotsky, M. O.; Thondorf, I.; Böhmer, V. *Angew. Chem., Int. Ed.* **2000**, *39*, 1264−1267. (b) Vysotsky, M. O.; Thondorf, I.; Böhmer, V. *Chem. Commun.* **2001**, 1890−1891.

(9) (a) Clark, T. D.; Ghadiri, M. R. *J. Am. Chem. Soc.* **1995**, *117*, 12364−12365. (b) Clark, T. D.; Kobayashi, K.; Ghadiri, M. R. *Chem.−Eur. J.* **1999**, *5*, 782−792. (c) Prins, L. J.; Verhage, J. J.; de Jong, F.; Timmerman, P.; Reinhoudt, D. N. *Chem.−Eur. J.* **2002**, *8*, 2302−2313.

(10) Prins, L. J.; Neuteboom, E. E.; Paraschiv, V.; Crego-Calama, M.; Timmerman, P.; Reinhoudt, D. N. *J. Org. Chem.* **2002**, *67*, 4808−4820.

(11) Prins, L. J.; De Jong, F.; Timmerman, P.; Reinhoudt, D. N. *Nature* **2000**, *408*, 181−184.

(12) Shi, X.; Fettinger, J. C.; Davis, J. T. *Angew. Chem., Int. Ed.* **2001**, *40*, 2827−2831.

(13) Ishi-i, T.; Crego-Calama, M.; Timmerman, P.; Reinhoudt, D. N.; Shinkai, S. *Angew. Chem., Int. Ed.* **2002**, *41*, 1924−1929.

(14) Cation recognition reviews: (a) Izatt, R. M.; Pawlak, K.; Bradshaw, J. S.; Bruening, R. L. *Chem. Rev.* **1995**, *95*, 2529−2586. (b) Izatt, R. M.; Pawlak, K.; Bradshaw, J. S.; Bruening, R. L. *Chem. Rev.* **1991**, *91*, 1721−2085.

(15) Anion coordination reviews: (a) Beer, P. D.; Gale, P. A. *Angew. Chem., Int. Ed.* **2001**, *40*, 487−516; b) Schimdtchen, F. P.; Berger, M. *Chem. Rev.* **1997**, *97*, 1609−1646.

(16) (a) Chrisstoffels, L. A. J.; de Jong, F.; Reinhoudt, D. N.; Sivelli, S.; Gazzola, L.; Casnati, A.; Ungaro, R. *J. Am. Chem. Soc.* **1999**, *121*, 10140−10151. (b) Kavallieratos, K.; Moyer, B. A. *Chem. Commun.* **2001**, 1620−1621. (c) Cafeo, G.; Gattuso, G.; Kohnke, F. H.; Notti, A.; Occhipinti, S.; Pappalardo, Parisi, M. F. *Angew. Chem., Int. Ed.* **2002**, *41*, 2122−2126.

(17) Ditopic receptor review: Kirkovits, G. J.; Shriver, J. A.; Gale, P. A.; Sessler, J. L. *J. Inclusion Phenom. Macrocyclic Chem.* **2001**, *41*, 69−75.

(18) Recent examples: (a) Deetz, M. J.; Shang M.; Smith B. D. *J. Am. Chem. Soc.* **2000**, *122*, 6201−6207. (b) Mahoney, J. M.; Beatty, A. M.; Smith, B. D. *J. Am. Chem. Soc.* **2001**, *123*, 5847−5848. (c) Wisner, J. A.; Beer, P. D.; Drew, M. G. B. *Angew. Chem., Int. Ed.* **2001**, *40*, 3606−3609. (d) Wisner, J. A.; Beer, P. D.; Berry, N. G.; Tomapatanaget, B. *Proc. Nat. Acad. Sci. U.S.A.* **2002**, *99*, 4983−4986.

(19) (a) Scheerder, J.; vanDuynhoven, J. P. M.; Engbersen, J. F. J.; Reinhoudt, D. N. *Angew. Chem., Int. Ed.* **1996**, *35*, 1090−1093. (b) Kubik, S. *J. Am. Chem. Soc.* **1999**, *121*, 5846−5855. (c) Beer, P. D.; Dent, S. W. *Chem. Commun.* **1998**, 825−826.

(20) The counterion can affect binding of its partner ion: (a) Kubik, S.; Goddard, R. *J. Org. Chem.* **1999**, *64*, 9475−9486. (b) Bartoli, S.; Roelens, S. *J. Am. Chem. Soc.* **1999**, *121*, 11908−11909. (c) Shukla, R.; Kida, T.; Smith, B. D. *Org. Lett.* **2000**, *2*, 3099−3101. (d) Arduini, A.; Giorgi, G.; Pochini, A.; Secchi, A.; Ugozzli, F. *J. Org. Chem.* **2001**, *66*, 8302−8308. (e) Bartoli, S.; Roelens, S. *J. Am. Chem. Soc.* **2002**, *124*, 8307−8315. (f) Arduini, A.; Brindani, E.; Giorgi, G.; Pochini, A.; Secchi, A. *J. Org. Chem.* **2002**, *67*, 6188−6194.

(21) Reviews on cation-templated self-assembly: (a) Linton, B.; Hamilton, A. D. *Chem. Rev.* **1997**, *97*, 1669−1680. (b) Leininger, S.; Olenyuk, B.; Stang, P. J. *Chem. Rev.* **2000**, *100*, 853−907.

(22) For a review on anion-templated self-assembly see: Vilar, R. *Angew. Chem., Int. Ed.* **2003**, *42*, 1460−1477.

(23) Severin and colleagues have described self-assembled ionophores made from coordination complexes that bind ion pairs: (a) Piotrowski, H.; Polborn, K.; Hilt, G.; Severin, K. *J. Am. Chem. Soc.* **2001**, *123*, 2699−2700. (b) Piotrowski, H.; Hilt, G.; Schulz, A.; Mayer, P.; Polborn, K.; Severin, K. *Chem.−Eur. J.* **2001**, *7*, 3196−3208. (c) Lehaire, M.-L.; Scopelliti, R.; Piotrowski, H.; Severin, K. *Angew. Chem., Int. Ed.* **2002**, *41*, 1419−1422. (d) Piotrowski, H.; Severin, K. *Proc. Nat. Acad. Sci. U.S.A.* **2002**, *99*, 4997−5000.

(24) (a) Forman, S. L.; Fettinger, J. C.; Pieraccini, S.; Gottarelli, G.; Davis, J. T. *J. Am. Chem. Soc.* **2000**, *122*, 4060−4067. (b) Shi, X. D.; Fettinger, J. C.; Davis, J. T. *J. Am. Chem. Soc.* **2001**, *123*, 6738−6739. (c) Kotch, F. W.; Fettinger, J. C.; Davis, J. T. *Org. Lett.* **2000**, *2*, 3277−3280.

(25) For some other papers on lipophilic G-quadruplexes and related structures, see: (a) Gottarelli, G.; Masiero, S.; Spada, G. *Chem. Commun.* **1995**, 2555−2557. (b) Davis, J. T.; Tirumala, S.; Jenssen, J. R.; Radler, E.; Fabris, D. *J. Org. Chem.* **1995**, *60*, 4167−4176. (c) Marlow, A. L.; Mezzina, E.; Spada, G. P.; Masiero, S.; Davis, J. T.; Gottarelli, G. *J. Org. Chem*, **1999**, *64*, 5116−5123. (d) Andrisano, V.; Gottarelli, G.; Masiero, S.; Heijne, E. H.; Pieraccini, S.; Spada, G. P. *Angew. Chem., Int. Ed.* **1999**, *38*, 2386-2388. (e) Sessler, J. L.; Sathiosatham, M.; Doerr, K.; Lynch, V.; Abboud, K. A. *Angew. Chem., Int. Ed.* **2000**, *39*, 1300−1303. (f) Kanie, K.; Yasuda, T.; Ujiie, S.; Kato, T *Chem. Commun.* **2000**, 1899−1900. (g) Cai, M.; Shi, X. D.; Sidorov, V.; Fabris, D.; Lam, Y.-F.; Davis, J. T. *Tetrahedron* **2002**, *58*, 661−671.

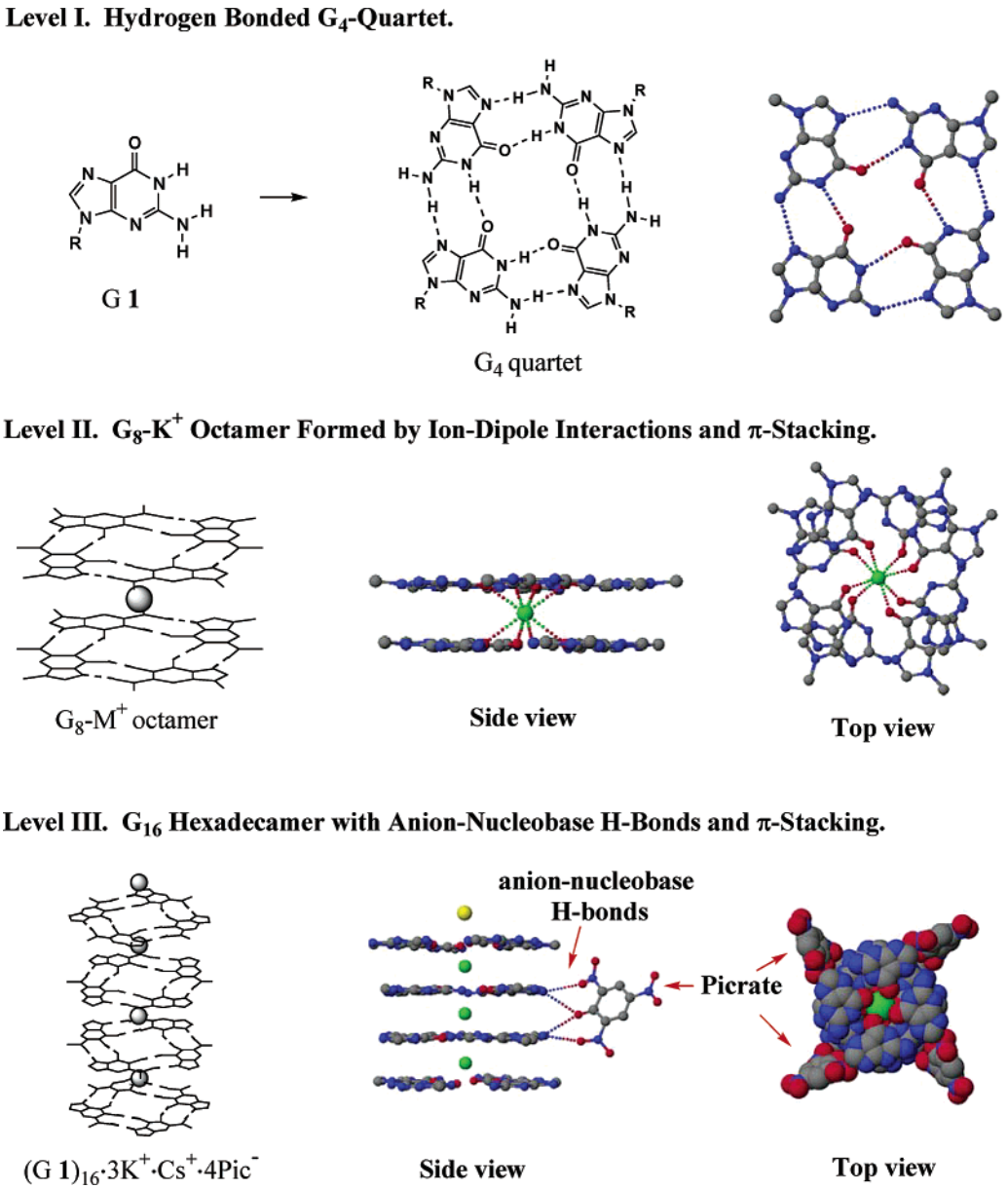

Figure 1. Hierarchical self-assembly to form the lipophilic G-quadruplex. The K^+ G-quadruplex (G **1**)$_{16}$·3K^+/Cs^+·4Pic$^-$, the original structure characterized by X-ray crystallography (ref 24a), is used to illustrate the different levels of self-organization. Level 3 shows the anion−nucleobase hydrogen-bonding interactions that are the focus of this study. For clarity, ribose units are omitted.

G_4-quartet via self-complementary H-bonds.[26] The G_4-quartets stack, using cation−dipole and aromatic−aromatic stacking interactions, to provide C_4-symmetric G_8·M^+ octamers with a cation sandwiched between the G_4-quartets. Four picrate anions use their phenolate oxygen atoms and their two ortho-substituted nitro groups to form bifurcated hydrogen bonds to the N2 H_B amino protons that project from the two "inner" G_4-quartets. These nucleobase−anion hydrogen bonds link two G_8·M^+ octamers together to give the D_4-symmetric hexadecamer. Thus, G **1** self-assembles to provide structures with cation and anion binding sites; the G-quadruplex has a cation-filled channel and grooves on its surface for anion recognition.

Single-crystal X-ray crystallography has shown that assemblies formed from G **1** and the divalent Ba^{2+} or Sr^{2+} picrate salts are also D_4-symmetric hexadecamers of formula (G **1**)$_{16}$·2M^{2+}·4Pic$^-$ (Scheme 1).[12,24b] We recently discussed the potential of these lipophilic G-quadruplexes to serve as ion pair receptors.[12] The G-quadruplex (G **1**)$_{16}$·2M^{2+}·4Pic$^-$ shown in Scheme 1 illustrates self-assembly's major advantage, namely, the efficient synthesis of ordered and functional structures. The G-quadruplex forms quantitatively by combining the components in an organic solvent. Twenty-two particles (16 nucleosides, 2 cations, and 4 anions) organize into a structure with dimensions of 25 × 30 × 30 Å and a molecular weight greater than 7900. But, as Raymond has noted,[27] "...although self-

(26) Leading references on cation-templated G-quartet formation by nucleotides: (a) Pinnavaia, T. J.; Marshall, C. L.; Mettler, C. M.; Fisk, C. L.; Miles, H. T.; Becker, E. D. *J. Am. Chem. Soc.* **1978**, *100*, 3625−3627. (b) Borzo, M.; Detellier, C.; Laszlo, P.; Paris, A. *J. Am. Chem. Soc.* **1980**, *102*, 1124−1134. (c) Detellier, C.; Laszlo, P. *J. Am. Chem. Soc.* **1980**, *102*, 1135−1141. (d) Bouhoutsos-Brown, E.; Marshall, C. L. Pinnavaia, T. J. *J. Am. Chem. Soc.* **1982**, *104*, 6576−6584. For G-quadruplex crystal structures from oligonucleotides see: (e) Phillips, K.; Dauter, Z.; Murchie, A. I.; Lilley, D. M. J.; Luisi, B. *J. Mol. Biol.* **1997**, *273*, 171−182. (f) Deng, J.; Xiong, Y.; Sundaralingam, M. *Proc. Nat. Acad. Sci. U.S.A.* **2001**, *98*, 13665−13670. (g) Horvath, M. P.; Schultz, S. C. *J. Mol. Biol.* **2001**, *310*, 367−377. (h) Parkinson, G. N.; Lee, M. P. H.; Neidle, S. *Nature* **2002**, *417*, 876−880.

Scheme 1. Lipophilic G-quadruplex (G **1**)$_{16}$·2Ba^{2+}·4Pic$^-$ Formed upon Self-Assembly of G **1**

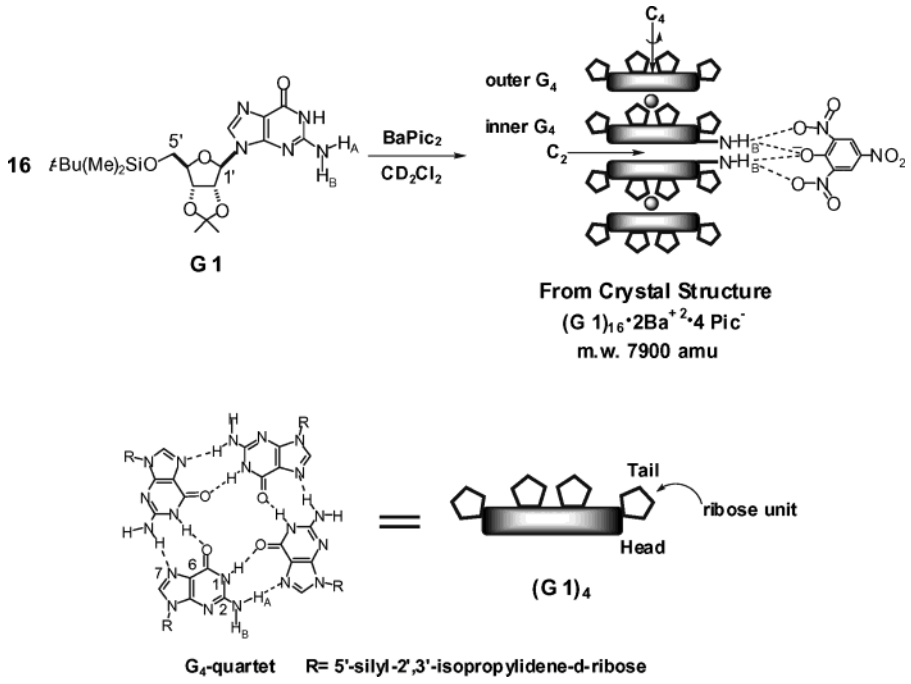

Chart 1. Anions (A$^-$) Used To Prepare Lipophilic G-Quadruplexes of Formula (G **1**)$_{16}$·2Ba^{2+}·4A$^-$

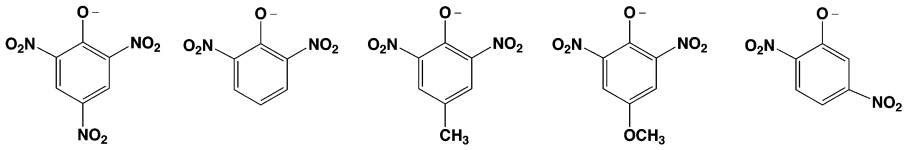

assembly represents a simple and efficient route to the construction of large, complex structures, understanding how this process works is not so straightforward." If we want to manipulate large synthetic assemblies, then learning how to control self-assembly and dynamic exchange is crucial. This paper focuses on defining the organic anion's role in G-quadruplex synthesis. One goal is to understand how components bound to the G-quadruplex influence assembly structure and dynamics. We show that the bound phenolate anions modulate the properties, particularly the kinetic stability, of these (G **1**)$_{16}$ hexadecamers.

Results and Discussion

In this study, we compare the structure and dynamics of five G-quadruplexes of formula (G **1**)$_{16}$·2Ba^{2+}·4A$^-$. Each complex contained Ba^{2+}, but differed in the bound nitrophenolate, 2,4,6-trinitrophenolate (picrate, **2**), 2,6-dinitrophenolate (2,6-DNP, **3**), 4-methyl-2,6-dinitrophenolate (4-Me-2,6-DNP, **4**),[28] 4-methoxy-2,6-dinitrophenolate (4-OMe-2,6-DNP, **5**), and 2,5-dinitrophenolate (2,5-DNP, **6**) (Chart 1). Although **2** is often considered to be a noncoordinating anion, its phenolate and nitro groups are hydrogen bond acceptors,[29] and its electron-deficient aromatic ring can π stack. Indeed, picrate has been shown to influence the structure and stability of ionophore−cation complexes.[12,30]

This paper is organized as follows. First, we review evidence that the G-quadruplex (G **1**)$_{16}$·2Ba^{2+}·4Pic$^-$ is a hexadecamer in the solid state and solution. We then describe mass spectrometry data that unequivocally support hexadecamer formation. Next, we present solid-state data showing that anion−quadruplex hydrogen bond distances are sensitive to anion structure and basicity. Then, we use NMR spectroscopy to show that G-quadruplexes with different anions possess markedly different kinetic stabilities in CD_2Cl_2. All the evidence indicates that the organic anion is crucial for controlling the properties of these cation-filled G-quadruplexes.

Solid-state structures for isomorphous G-quadruplexes (G **1**)$_{16}$·2Ba^{2+}·4Pic$^-$ and (G **1**)$_{16}$·2Sr^{2+}·4Pic$^-$ indicated that self-assembly of G **1** and the metal picrates gave a hexadecamer.[12,24b] We previously described NMR experiments that provided strong evidence that a hexadecamer, as opposed to a dissociated octamer, (G **1**)$_8$·Ba^{2+}, was the major species in CD_2Cl_2 solution. Thus, a 1:1 mixture of (G **1**)$_{16}$·2Ba^{2+}·4Pic$^-$ and (G **1**)$_{16}$·2Sr^{2+}·4Pic$^-$ equilibrated to give a statistical 1:1:2 ratio of the starting hexadecamers and the "mixed" hexadecamer (G **1**)$_8$·Ba^{2+}·(G **1**)$_8$·Sr^{2+}·4Pic$^-$, an isomerization product formed

(27) Davis, A. V.; Yeh, R. M.; Raymond, K. N. *Proc. Natl. Acad. Sci. U.S.A.* **2002**, *99*, 4793−4796.
(28) Cotelle, P.; Catteau, J. P. *Synth. Commun.* **1996**, *26*, 4105−4112.
(29) (a) Etter, M. C. *Acc. Chem. Res.* **1990**, *23*, 120−126. (b) Etter, M. C. *J. Phys. Chem.* **1991**, *95*, 4601−4610. (c) Robinson, J. M. A.; Philp, D.; Harris, K. D. M.; Kariuka, B. M. *New J. Chem.* **2000**, *24*, 799−806.
(30) (a) Harrowfield, J. *J. Chem Soc., Dalton Trans.* **1996**, 3165−3171. (b) Böhmer, V.; Dalla-Cort, A.; Mandolini, L. *J. Org. Chem.* **2001**, *66*, 1900−1902. (c) Talanova, G. G.; Elkarim, N. S. A.; Talanov, V. S.; Hanes, R. E.; Hwang, H. S.; Bartsch, R. A.; Rogers, R. D. *J. Am. Chem. Soc.* **1999**, *121*, 11281−11290.

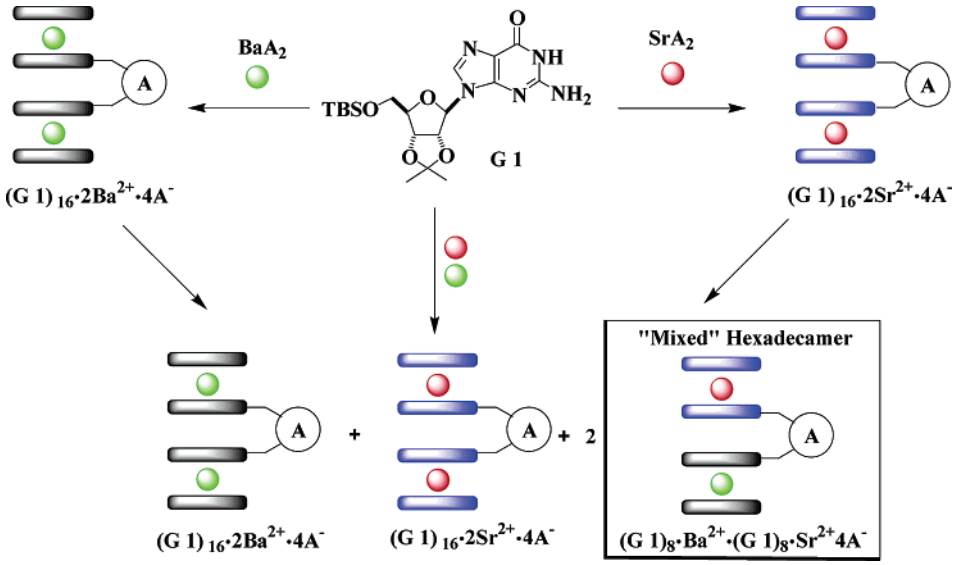

Figure 2. A series of ^{1}H NMR experiments (see ref 12) showed that self-assembly of G **1** with a 1:1 mixture of Ba^{2+} and Sr^{2+} salts gives a statistical 1:1:2 mixture of the hexadecameric G-quadruplexes (G **1**)$_{16}$·2Ba^{2+}·4A^- and (G **1**)$_{16}$·2Sr^{2+}·4A^-, and the mixed hexadecamer (G **1**)$_8$·Ba^{2+}·(G **1**)$_8$·Sr^{2+}·4A^-. The mixed hexadecamer is an isomerization product from formal exchange of (G **1**)$_8$·M^{2+} octamers between (G **1**)$_{16}$·2Ba^{2+}·4A^- and (G **1**)$_{16}$·2Sr^{2+}·4A^-. The nitrophenolate anions, A^-, that bridge the octamer units in these hexadecameric G-quadruplexes are shown in Chart 1.

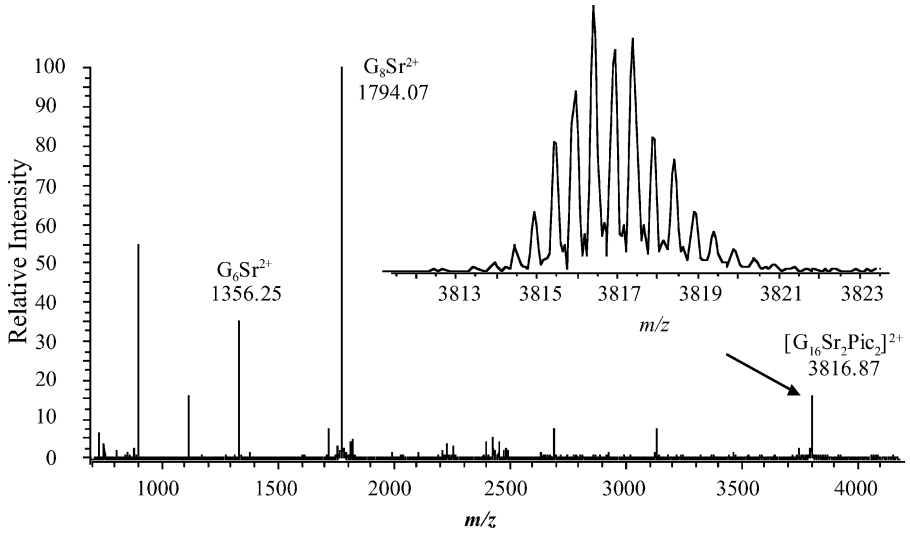

Figure 3. ESI-MS provides direct evidence for the formation of hexadecameric G-quadruplex from G **1**. The inset shows the high-resolution spectrum of [(G **1**)$_{16}$·2Sr^{2+}·2Pic^-]$^{2+}$.

by formal exchange of (G **1**)$_8$·M^{2+} octamers between (G **1**)$_{16}$·2Ba^{2+}·4Pic^- and (G **1**)$_{16}$·2Sr^{2+}·4Pic^- (Figure 2). To gain more direct evidence for hexadecameric G-quadruplexes in solution, we turned to electrospray mass spectrometry.

Mass Spectrometry Evidence for the Guanosine Hexadecamer. ESI-MS, a powerful method for biomolecular analysis,[31] is also a key characterization technique in supramolecular chemistry.[32] Since cations are an integral part of the G-quadruplexes, their ESI-MS analysis does not require any ion labeling steps.[33] As shown in Figure 3, ESI-FTICR-MS analysis of a CH_3CN solution of (G **1**)$_{16}$·2Sr^{2+}·4Pic^- gave a significant peak at *m*/*z* 3816.87, characteristic of a hexadecamer, [(G **1**)$_{16}$·2Sr^{2+}·2Pic^-]$^{2+}$, that had lost two picrate anions. The Figure 3 inset shows the isotopic resolution of this species, confirming it as a doubly charged hexadecamer. Furthermore, mixing (G **1**)$_{16}$·2Ba^{2+}·4Pic^- and (G **1**)$_{16}$·2Sr^{2+}·4Pic^- in CH_3CN provided three doubly charged peaks in the *m*/*z* 3800 region (Figure 4), corresponding to the starting complexes and the mixed hexadecamer [(G **1**)$_8$·Ba^{2+}·(G **1**)$_8$·Sr^{2+}·2Pic^-]$^{2+}$. The signal for [(G **1**)$_8$·Ba^{2+}·(G **1**)$_8$·Sr^{2+}·2Pic^-]$^{2+}$ is consistent with the species proposed in previous NMR experiments, an isomerization product arising from formal (G **1**)$_8$·M^{2+} octamer exchange between (G **1**)$_{16}$·2Ba^{2+}·4Pic^- and (G **1**)$_{16}$·2Sr^{2+}·4Pic^-.[12] These ESI-MS results confirm formation of a hexadecameric G-quadruplex from G **1** and picrate salts in organic solvents.

(31) (a) Siuzdak, G. *Proc. Natl. Acad. Sci. U.S.A.* **1994**, *91*, 11290−11297. (b) Hofstadler, S. A.; Griffey, R. H. *Chem. Rev.* **2001**, *101*, 377−390.
(32) (a) Schalley, C. A. *J. Int. Mass Spectrom.* **2000**, *134*, 11−39. (b) Schalley, C. A. *Mass Spectom. Rev.* **2001**, *20*, 253−309. (c) Manna, J.; Kuehl, C. J.; Whiteford, J. A.; Stang, P. J.; Muddiman, D. C.; Hofstadler, S. A.; Smith, R. D. *J. Am. Chem. Soc.* **1997**, *119*, 11611−11619.
(33) Other G-quartet ESI-MS studies: (a) Fukushima, K.; Iwahashi, H. *Chem. Commun.* **2000**, 895−896. (b) Manet, I.; Francini, L.; Masiero, S.; Pierracinni, S.; Spada, G. P.; Gottarelli, G. *Helv. Chim. Acta* **2001**, *84*, 2096−2107. (c) Koch, K. J.; Aggerholm, T.; Nanita, S. C.; Cooks, R. G. *J. Mass Spectrom.* **2002**, *37*, 676−686. (d) Aggerholm, T.; Nanita, S. C.; Koch, K. J: Cooks, R. G. *J. Mass Spectrom.* **2003**, *38*, 87−97. (e) Sakamoto, S.; Nakatani, K.; Saito, I.; Yamaguchi, K. *Chem. Commun.* **2003**, 788−789.

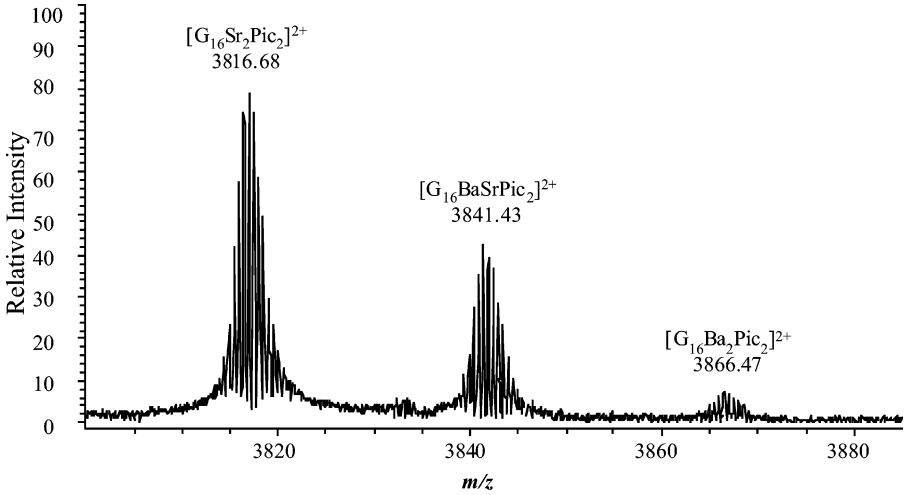

Figure 4. ESI-MS confirmed formation of the mixed hexadecamer $[(G\ \mathbf{1})_8{\cdot}Ba^{2+}{\cdot}(G\ \mathbf{1})_8{\cdot}Sr^{2+}{\cdot}2Pic^-]^{2+}$ as indicated by the peak at *m*/*z* 3841.43. The sample was prepared by dissolving recrystallized G-quadruplexes $(G\ \mathbf{1})_{16}{\cdot}2Ba^{2+}{\cdot}4Pic^-$ and $(G\ \mathbf{1})_{16}{\cdot}2Sr^{2+}{\cdot}4Pic^-$ in CH_3CN.

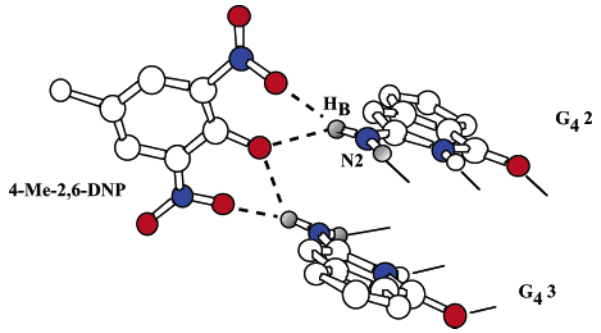

Figure 5. Anion−nucleobase hydrogen bond interactions from the crystal structure of $(G\ \mathbf{1})_{16}{\cdot}2Ba^{2+}{\cdot}4(\mathbf{4})$.

Table 1. Nucleobase−Anion H-Bond Distances (Å) in the G-Quadruplexes $(G\ \mathbf{1})_{16}{\cdot}2Ba^{2+}{\cdot}4A^-$

		2[a]	3	4	5	6[b]
Inner G_4 A	N(2)···O phenol	3.005(11)	2.900(7)	2.905(9)	2.896(8)	none
	N(2)···ONO	3.171(13)	3.040(9)	3.116(9)	3.041(8)	3.02
Inner G_4 B	N(2)···O phenol	2.948(12)	3.025(7)	2.930(9)	2.915(8)	2.80
	N(2)···ONO	3.063(14)	3.063(8)	3.016(8)	2.9775(9)	none
	av N(2)···O phenol	2.98	2.94	2.92	2.91	2.80
	av N(2)···ONO	3.12	3.07	3.07	3.01	3.02

[a] Values for $(G\ \mathbf{1})_{16}{\cdot}2Ba^{2+}{\cdot}4Pic^-$ were obtained from the published crystal structure in ref 12. [b] Mean values for the two separate G-quadruplexes in the unit cell. In addition, six of the eight anions in the unit cell of $(G\ 1)_{16}{\cdot}2Ba^{2+}{\cdot}4(\mathbf{6})$ showed considerable disorder between the two possible anion−nucleobase hydrogen bond orientations.

G-Quadruplex Crystal Structures. Previous crystal structures for $(G\ \mathbf{1})_{16}{\cdot}2Ba^{2+}{\cdot}4Pic^-$ and $(G\ \mathbf{1})_{16}{\cdot}2Sr^{2+}{\cdot}4Pic^-$ revealed that four picrate anions fit into grooves on the G-quadruplex surface.[12,24b] The picrate anions are anchored by hydrogen bonds to the exocyclic N2 amino groups that extend from the two inner G_4-quartets. The anion's phenoxide hydrogen bonds to both N2 amino groups, while the picrate's *o*-nitro groups each provide another oxygen atom for hydrogen bonding to the N2 H_B protons (Figure 5). Overall, four picrate anions cross-link two $(G\ \mathbf{1})_8{\cdot}Ba^{2+}$ octamers by forming hydrogen bonds with the inner two G-quartet layers. This nucleobase−anion hydrogen bonding arises because of other interdependent interactions, since it is cation coordination, G_4-quartet formation, and quartet stacking that orient the N2 amino groups for anion recognition.

To better define the anion's influence on G-quadruplex structure and dynamics, we prepared single crystals of four new Ba^{2+} G-quadruplexes using G **1**; each new complex contained different dinitrophenolates as the counterions. We chose the 2,6-dinitrophenolate anions **3**−**5** to compare with **2** to evaluate whether the anion's electronic properties influence G-quadruplex structure and dynamics. Earlier work used a G-quadruplex picrate complex, $(G\ \mathbf{1})_{16}{\cdot}2Ba^{2+}{\cdot}4Pic^-$, containing a 2,6-dinitrophenolate with an electron-withdrawing *p*-nitro group.[12,24b]

The present study provided analogous G-quadruplexes with an anion lacking a para substituent (**3**) and with anions containing electron-donating substituents (*p*-Me and *p*-OMe, **4** and **5**). The anion **6** was chosen to compare with its isomer **3** to test whether the anion's chelating ability is an important feature in stabilizing the lipophilic G-quadruplex. **6** (the conjugate acid has $pK_a = 5.22$)[34] is more basic than **3** (the conjugate acid has $pK_a = 3.96$),[34] but **6** cannot form the same bifurcated hydrogen bonds with the inner G_4-quartets as **3**.

Extracting a water solution of the Ba^{2+} dinitrophenolates **3**−**5** with a $CDCl_3$ solution of G **1** generated the G-quadruplexes. In all cases, the ^1H NMR spectra indicated quantitative formation of $(G\ \mathbf{1})_{16}{\cdot}2Ba^{2+}{\cdot}4A^-$. Single crystals of the complexes were grown and structures determined for $(G\ \mathbf{1})_{16}{\cdot}2Ba^{2+}{\cdot}4(\mathbf{3})$, $(G\ \mathbf{1})_{16}{\cdot}2Ba^{2+}{\cdot}4(\mathbf{4})$, $(G\ \mathbf{1})_{16}{\cdot}2Ba^{2+}{\cdot}4(\mathbf{5})$, and $(G\ \mathbf{1})_{16}{\cdot}2Ba^{2+}{\cdot}4(\mathbf{6})$. Although each new complex had its own large and unique unit cell (for crystallography data see Tables 1−5 in the Supporting Information), all of the crystal structures revealed similar hexadecameric G-quadruplexes consisting of four layers of stacked G_4-quartets binding two coaxial Ba^{2+} cations. Key structural data for these new complexes, along with previous values for $(G\ \mathbf{1})_{16}{\cdot}2Ba^{2+}{\cdot}4Pic^-$,[12] are listed in Table 1 and in Tables 6 and 7 in the Supporting Information.

Crystal structures of four related assemblies with *o*-nitro groups, $(G\ \mathbf{1})_{16}{\cdot}2Ba^{2+}{\cdot}4(\mathbf{2})$,[12] $(G\ \mathbf{1})_{16}{\cdot}2Ba^{2+}{\cdot}4(\mathbf{3})$, $(G\ \mathbf{1})_{16}{\cdot}2Ba^{2+}{\cdot}4(\mathbf{4})$, and $(G\ \mathbf{1})_{16}{\cdot}2Ba^{2+}{\cdot}4(\mathbf{5})$, indicate that the G-quadruplex dimensions, such as G_4-quartet H-bond distances and G_4-quartet separations, do not vary much with the anion's identity (see the Supporting Information). But, there are obvious geometric differences involving the anion−nucleobase H-bond distances within this series (Table 1). In all four structures, the anion's

(34) Lagier, C. M.; Oliveieri, A. C.; Harris, R. K. *J. Chem. Soc., Perkin Trans. 2* **1998**, 1791−1796.

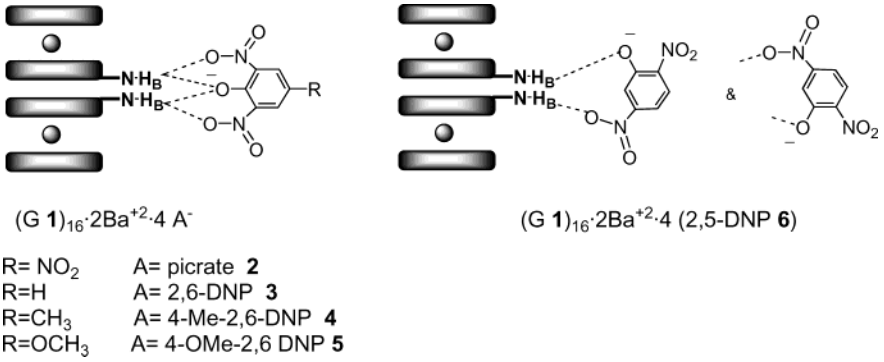

Figure 6. Schematic representation of the anion−nucleobase hydrogen bonding as determined from crystal structures of lipophilic G-quadruplexes (G **1**)$_{16}$·2Ba^{2+}·4A^{-}. Unlike tridentate 2,6-dinitrophenolate anions **2**−**5** that form a bifurcated H-bond network with the N2 H$_B$ amino protons of the inner G$_4$-quartets, the anion **6** forms just two anion−nucleobase hydrogen bonds. In the crystal structure of (G **1**)$_{16}$·2Ba^{2+}·4(**6**) the disordered anions show two major hydrogen bond geometries.

phenolate oxygen and two nitro groups hydrogen bond with the N2 H$_B$ protons of the inner G$_4$-quartets (Figure 5). These anion−nucleobase hydrogen bonds shorten as the anion is changed from **2** to **3** to the more basic **4** and **5**. Thus, the average distance for the anion nitro−G-quadruplex hydrogen bonds shortens by more than 0.1 Å, from 3.12 Å for (G **1**)$_{16}$·2Ba^{2+}·4(**2**) to 3.01 Å for the G-quadruplex with **5**. Since the structures are determined to a resolution of about 0.01 Å, this 0.1 Å change in hydrogen bond distance is a significant change. There is similar shortening of the phenoxide−N2 nucleobase hydrogen bonds. The average N(2)···O distance shortens by 0.07 Å, from 2.98 Å for (G **1**)$_{16}$·2Ba^{2+}·4(**2**) to 2.91 Å for (G **1**)$_{16}$·2Ba^{2+}·4(**5**). This progressive shortening of the anion−nucleobase hydrogen bond distances correlates with an increase in phenolate basicity. The longer anion−nucleobase hydrogen bonds for (G **1**)$_{16}$·2Ba^{2+}·4Pic^{-} suggest that **2** is held less tightly to the G-quadruplex than are the more electron-rich anions such as **3**−**5**.

The crystal structure of the fifth complex, (G **1**)$_{16}$·2Ba^{2+}·4(**6**), also revealed some significant anion-dependent changes. Unlike the 2,6-dinitrophenolate analogues **2**−**5**, which all form tridentate hydrogen-bonding interactions with the inner G$_4$-quartets (Figure 6A), the anion **6** forms only bidentate contacts with the G-quadruplex. Moreover, in the crystal structure of (G **1**)$_{16}$·2Ba^{2+}·4(**6**), the phenoxide oxygen of the 2,5-DNP anion does not bridge separate G$_4$-quartet amino groups. Instead, the 2,5-DNP's phenoxide hydrogen bonds to only one of the inner G$_4$-quartet amino groups, while the anion's *m*-nitro group hydrogen bonds to the other N2 amino group (Figure 6B). Furthermore, a number of the anions in this particular structure were highly disordered, indicating that **6** is not as tightly bound to the G-quadruplex as are the other anions **2**−**5**. Overall, crystallographic analysis of the five Ba^{2+} G-quadruplexes reveals some key structural differences. While G-quadruplex dimensions vary little, the anion−nucleobase hydrogen bond geometry does change as a function of phenolate basicity and structure. As described below, the bound anion also influences G-quadruplex solution properties.

^{1}H NMR Spectra of Different G-Quadruplexes. The final sections of this paper focus on the solution properties of these G-quadruplexes, and some key data from these studies are summarized in Table 2. The first indication that the anion modulates the solution properties of Ba^{2+} G-quadruplexes came from comparing ^{1}H NMR spectra in CD_2Cl_2. Crystal structures had shown that the N2 H$_B$ amino proton of the inner G$_4$-quartets

Table 2. Key Solution Data Concerning the Anion's Role in G-Quadruplex Structure and Dynamics

anion	phenol pK_a[a]	δ(NH$_{2B}$) (ppm)	anion exchange rate[b] (s^{-1})	"isomerization" half-life[d]
2	0.38	7.42	16 ± 1	42 h
3	3.96	8.11	2.3 ± 0.2	≫2 months
4		8.17	nd	nd
5		8.18	1.9 ± 0.2	nd
6	5.22	8.12	>30[c]	30 min

[a] From ref 34. [b] Determined from EXSY NMR at −10 °C in CD_2Cl_2. [c] Lower limit calculated from 1D NMR spectra at −10 °C in CD_2Cl_2. [d] See the text and Figures 9 and 10 for pertinent information.

coordinates to the phenolate anion. NMR chemical shifts for the inner G$_4$-quartet's N2 H$_B$ proton appear sensitive to the strength of this anion−nucleobase hydrogen bond (Figure 7 and Table 2). For these G-quadruplexes, two sets of ^{1}H NMR resonances are observed in CD_2Cl_2, corresponding to signals for the "inner" and "outer" G$_4$-quartets. The ^{1}H NMR spectra for complexes containing different 2,6-dinitrophenolate anions (**2**−**5**) are similar, with the only major difference occurring for the inner G$_4$-quartet's N2 H$_B$ signal. In these complexes, well-separated and sharp signals for the inner amino protons (N2 H$_A$ and N2 H$_B$) were present. As illustrated in Figure 7, the inner N2 H$_B$ signal for (G **1**)$_{16}$·2Ba^{2+}·4(**3**), at δ 8.11, is shifted far downfield ($\Delta\delta$ = + 0.69 ppm) relative to the N2 H$_B$ resonance in the picrate complex (G **1**)$_{16}$·2Ba^{2+}·4Pic^{-} (δ 7.42). The G-quadruplexes with electron-donating groups in the 2,6-dinitrophenolate's para position, (G **1**)$_{16}$·2Ba^{2+}·4(**4**) and (G **1**)$_{16}$·2Ba^{2+}·4(**5**), have sharp and distinct N2 H$_B$ signals that are shifted even further downfield, to δ 8.17 and δ 8.18, respectively. These comparative NMR data are consistent with the more basic anions **3**−**5**, all forming stronger H-bonds with the inner G$_4$-quartets than does **2**.

The ^{1}H NMR spectrum for (G **1**)$_{16}$·2Ba^{2+}·4(**6**) was different from spectra for the other G-quadruplexes (Figure 7c). In (G **1**)$_{16}$·2Ba^{2+}·4(**6**) the N2 H$_B$ resonance was still significantly downfield shifted ($\Delta\delta$ = + 0.80 ppm), relative to the same signal in the picrate complex. However, instead of two sharp signals for the inner G$_4$-quartet's N2 amino protons, the G-quadruplex containing **6** had broadened resonances for both N2 H$_A$ and N2 H$_B$ at room temperature. These increased NMR line widths suggest either faster anion exchange or faster C2−N2 bond rotation (or both) in (G **1**)$_{16}$·2Ba^{2+}·4(**6**) relative to (G **1**)$_{16}$·2Ba^{2+}·4(**3**). Recall that the crystal structure of (G **1**)$_{16}$·2Ba^{2+}·4(**6**) had shown that **6** does not cross-link the inner G$_4$-

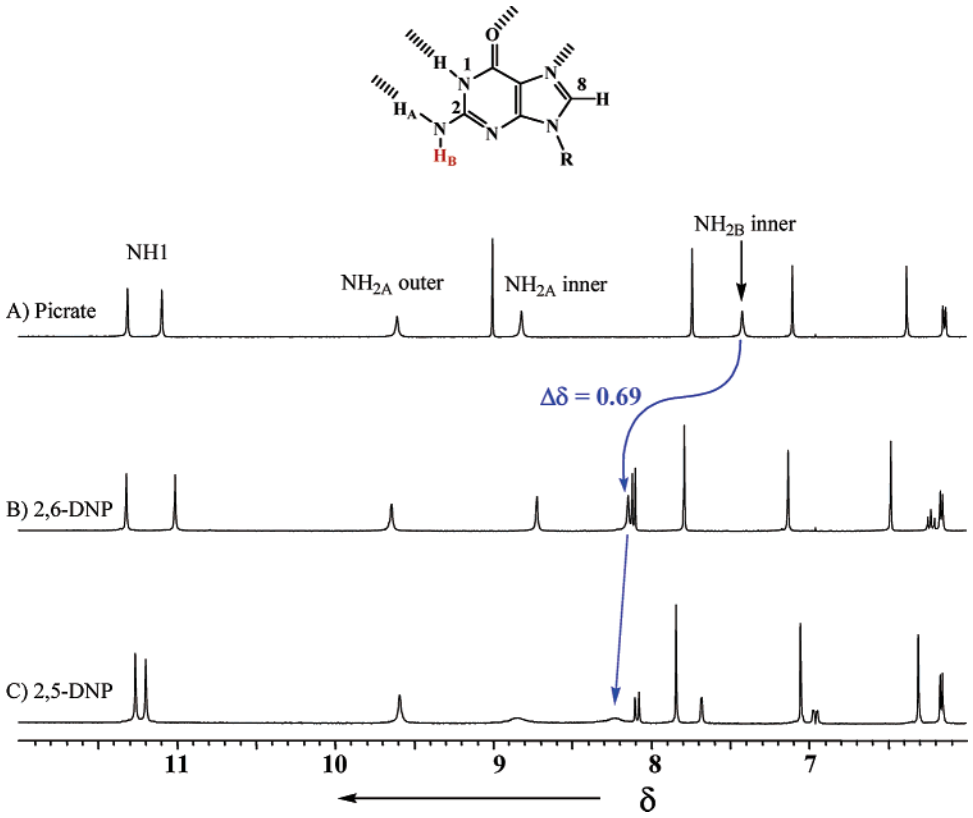

Figure 7. ^{1}H NMR (400 MHz) spectra for Ba^{2+} G-quadruplexes with different anions. Samples were made by dissolving crystalline complexes in CD_2Cl_2 at room temperature: (A) (G **1**)$_{16}$·2Ba^{2+}·4(**2**); (B) (G **1**)$_{16}$·2Ba^{2+}·4(**3**) (relative to spectrum A the inner G_4-quartet's amino proton N2 H_{2B} underwent a significant downfield shift ($\Delta\delta = +0.69$ ppm)); (C) (G **1**)$_{16}$·2Ba^{2+}·4(**6**) (relative to spectra A and B, the inner G_4-quartet's amino protons N2 H_A and H_B were significantly broadened in this complex).

quartets nearly as effectively as does **3** (Figure 6). We attribute the significantly broadened N2 H_A/H_B resonances for (G **1**)$_{16}$·2Ba^{2+}·4(**6**) to a "looser" binding of the **6** anion (as compared to **3**) to the G-quadruplex amino groups. In other words, the **6** anion is less restricted than **3** when binding to the G-quadruplex surface, and therefore, the G-quartet amino group shows increased dynamics, as reflected in their broader NMR signals.[35] Overall, these major differences in NMR chemical shifts and line shapes for the inner G-quartet's amino group as a function of the bound anion are compelling evidence that the anions are important components of G-quadruplex solution structure. Finally, more support for the anion's role in stabilizing the hexadecameric structure came from extraction experiments using $Na^+Ph_4B^-$ and $K^+Ph_4B^-$. Extraction of these tetraphenylborate salts from water into $CHCl_3$ by G **1** gave poorly resolved ^{1}H NMR spectra, indicating ill-defined aggregates. Tetraphenylborate anions, unlike phenolates **2**−**6**, cannot bridge the inner G-quartet's amino groups; these qualitative data support the notion that the hexadecameric G-quadruplex structure is mediated by ion pair binding. As described below, both the nitrophenolate anion's basicity and its ability to form bifurcated hydrogen bonds with the G-quadruplex modulate the solution dynamics of these complexes.

Anion Exchange and Kinetic Stability of the G-Quadruplexes. The combined data from our solid-state structures (H-bond distances) and NMR solution studies (NH_B chemical shift and line width changes) suggested that the G-quadruplex binds some anions more tightly than other anions. To obtain more quantitative information, we also used 2D EXSY NMR[36] experiments to measure the exchange rates for three different anions in CD_2Cl_2, namely, **2**−**5**. These anions, which all chelate the inner G_4 quartets of (G **1**)$_{16}$·2Ba^{2+}·4A^- G-quadruplexes, give separate signals for bound and free species at equilibrium. In contrast, even at −10 °C in CD_2Cl_2 the anion **6** is in fast exchange on the NMR chemical shift time scale between its bound and free states, an indication that **6** binds less tightly to the G-quadruplex than do anions **2**−**5** (a lower limit of $k > 30$ s^{-1} was calculated for 1 mM **6** at −10 °C, Table 2). EXSY NMR provides information on chemical exchange in the millisecond to second time regime, and it is widely used to study the dynamics of self-assembled systems.[37,38] By comparing different Ba^{2+} G-quadruplexes, we gained further insight into the "tightness" [35] of the G-quadruplex−anion interactions. "Free" anions were generated by complexing barium nitrophenolate salts with [2.2.2]cryptand. In this way, the phenolates were separated from the caged Ba^{2+} cations.[39] We prepared

(35) For a discussion of the relationship between kinetic barriers and the structural ordering of noncovalent hydrogen-bonded assemblies, see: (a) O'Brien, S. W.; Shiozawa, H.; Zerella, R.; O'Brien, D. P.; Williams, D. H. *Org. Biomol. Chem*. **2003**, *1*, 472−477. (b) Williams, D. H.; O'Brien, D. P.; Bardsley, B. *J. Chem. Soc., Perkin Trans. 2* **2000**, 1681−1685.

(36) Perrin, C. L.; Dwyer, T. J. *Chem. Rev.* **1990**, *90*, 935−967.

(37) For a review see: Pons, M.; Millet, O. *Prog. Nucl. Magn. Reson. Spectrosc*. **2001**, *38*, 267.

(38) For a recent application of EXSY in molecular recognition studies, see: (a) Mögck, O.; Pons, M.; Böhmer, V.; Vogt, W. *J. Am. Chem. Soc.* **1997**, *119*, 5706−5712. (b) Söntjens, S. H. M.; Sijbesma, R. P.; van Genderen, M. H. P.; Meijer, E. W. *J. Am. Chem. Soc.* **2000**, *122*, 7487−7493. (c) Saudan, C.; Dunand, F. A.; Abou-Hamdan, A.; Bugnon, P.; Lye, P. G.; Lincoln, S. F.; Merbach, A. E. *J. Am. Chem. Soc.* **2001**, *123*, 10290−10298. (d) Chang, S. Y.; Choi, J. S.; Jeong, K. S. *Chem.—Eur. J.* **2001**, *7*, 2687−2697.

(39) Lehn, J. M.; Sauvage, J. P. *J. Am. Chem. Soc.* **1975**, *97*, 6700−6707.

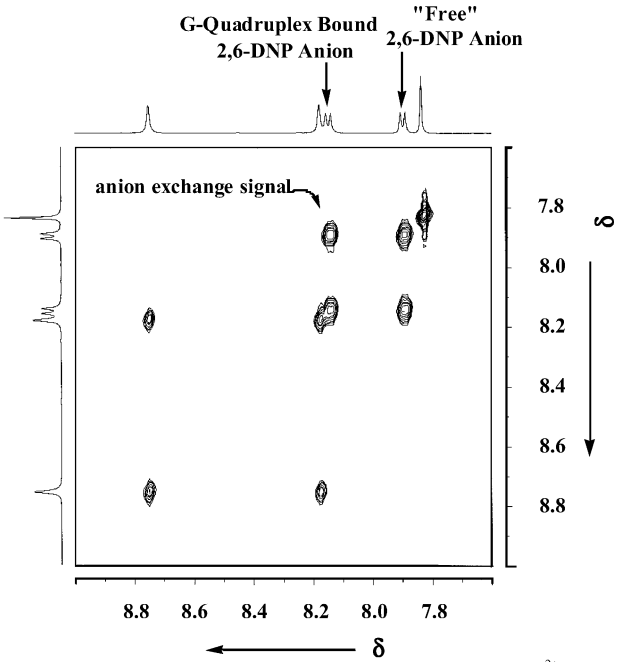

Figure 8. A portion of the EXSY NMR spectrum of a 1:2 mixture of (G **1**)$_{16}$·2Ba^{2+}·4(**3**) and [[2.2.2]cryptand·Ba^{2+}]·2(**3**). The experiment was done at −10 °C in CD_2Cl_2 with τ_m = 80 ms. EXSY experiments provided rate constants for exchange between G-quadruplex bound anion and free anion.

samples in CD_2Cl_2 that contained a 1:1 ratio of bound and free anions by combining (G **1**)$_{16}$·2Ba^{2+}·4A$^-$ with 2 equiv of the cryptate complex [[2.2.2]cryptand·Ba^{2+}]·2A$^-$. In the 1D ^{1}H NMR spectra, separate signals were observed for the bound and free anions. All EXSY NMR experiments used samples that were 1 mM in G-quadruplex in CD_2Cl_2 at −10 °C with a mixing time of τ_m= 80 ms. After integration of the off-diagonal exchange cross-peaks and the on-diagonal peaks (Figure 8), we extracted the anion exchange rate constants (k) for three G-quadruplexes, (G **1**)$_{16}$·2Ba^{2+}·4(**2**), (G **1**)$_{16}$·2Ba^{2+}·4(**3**), and (G **1**)$_{16}$·2Ba^{2+}·4(**5**) by assuming two-site exchange and using eq 1.[36]

$$k = \frac{\ln[(R+1)/(R-1)]}{\tau_m} \qquad R = I_{diagonal}/I_{cross} \qquad (1)$$

As summarized in Table 2, EXSY experiments indicated that the anion exchange rate constant is approximately 7 times faster for (G **1**)$_{16}$·2Ba^{2+}·4(**2**) ($k = 16 \pm 1$ s^{-1}) than for the complexes containing the more basic anions, namely, **3** ($k = 2.3 \pm 0.2$ s^{-1}) and **5** ($k = 1.9 \pm 0.2$ s^{-1}). Although there was not a linear free energy relationship between exchange rates and phenolate's Hammett constant,[40] anion exchange between bound and free states is clearly related to the strength of the G-quadruplex−anion interaction. The stronger bases **3** and **5** exchange more slowly with the bound anions than does the picrate anion **2**.

To summarize, NMR spectroscopy shows that the anion **6**, when free in solution, exchanges faster with its G-quadruplex-bound anion than any of the 2,6-dinitro-substituted phenolates **2**−**5**. The increased lability of **6** is likely due to weaker anion−nucleobase hydrogen bonds, since the bidentate **6** is less effective than the tridentate 2,6-dinitrophenolate anions **2**−**5** at bridging the inner G_4-quartets. Importantly, anion **2** is bound more tightly to the G-quadruplex than is anion **6**, even though **6** (pK_a 5.22) is a much stronger base than **2** (pK_a 0.38) by a factor of over 80000. Thus, the anion's structure and its chelating ability are important. We conclude that the *o*-nitro groups in anions **2**−**5** must be significant hydrogen bond acceptors for the guanine N2 H_B protons that extend into solution.[41] For complexes containing 2,6-dinitrophenolate anions, electronic effects further modulate the kinetic stability of the G-quadruplex. Thus, EXSY data shows that **3** and **5** bind more tightly to the G-quadruplex than does the less basic **2**. So, both the ability to form bifurcated H-bonds (a structural effect) and the anion's basicity (an electronic effect) influence the tightness of anion binding to the lipophilic G-quadruplex.

Anion Binding Controls the Dynamics of Self-Assembled G-Quadruplexes. This section describes the anion's effect on a supramolecular isomerization. Previously, we showed that equimolar amounts of two G-quadruplexes differing in their cation, (G **1**)$_{16}$·2Ba^{2+}·4A$^-$ and (G **1**)$_{16}$·2Sr^{2+}·4A$^-$, equilibrated in CD_2Cl_2 to give a statistical 1:1:2 mixture of (G **1**)$_{16}$·2Ba^{2+}·4A$^-$, (G **1**)$_{16}$·2Sr^{2+}·4A$^-$, and the rearranged product, mixed hexadecamer (G **1**)$_8$·Ba^{2+}·(G **1**)$_8$·Sr^{2+}·4A$^-$ (Figure 2).[12] A D_4-symmetric hexadecamer, such as (G **1**)$_{16}$·2Ba$_2^{2+}$·4Pic$^-$ or (G **1**)$_{16}$·2Sr^{2+}·4Pic$^-$, has only two sets of NMR signals, one set for the two degenerate inner G_4-quartets and one set for degenerate outer G_4-quartets. In contrast, the lower symmetry hexadecamer (G **1**)$_8$·Ba^{2+}·(G **1**)$_8$·Sr^{2+}·4Pic$^-$ shows four sets of NMR signals for its nonequivalent G-quartet layers. With picrate as anion, this isomerization occurred with $t_{1/2}$ = 42 h for a 1 mM solution in CD_2Cl_2 at room temperature.[12]

From the EXSY NMR experiments, we had established that **2** ($k = 16 \pm 1$ s^{-1}) is more tightly bound to the G-quadruplex than is **6** ($k > 30$ s^{-1}), despite the fact that it is a much weaker base than **6**. Thus, we expected that the mixtures of Ba^{2+} and Sr^{2+} G-quadruplexes containing **6** should isomerize faster than those containing **2** if anion dissociation is part of the isomerization's rate-limiting step. We studied these isomerization reactions in CD_2Cl_2, using 1:1 mixtures of the appropriate Ba^{2+} and Sr^{2+} G-quadruplexes. The ^{1}H NMR spectra for various mixing experiments in Figure 9 show the diagnostic H8 region. A mixture of (G **1**)$_{16}$·2Ba^{2+}·4(**6**) and (G **1**)$_{16}$·2Sr^{2+}·4(**6**) isomerizes much faster ($t_{1/2}$ = 30 min) than G-quadruplexes containing **2** ($t_{1/2}$ = 42 h). Clearly, **2** must strengthen the cross-linking of inner G_4-quartets, relative to **6**, leading to the significant increase in the G-quadruplex kinetic stability.

The use of a more basic and chelating anion, namely, **3**, resulted in extraordinary kinetic stabilization of the G-quadruplex. Experiments in Figure 10 indicate that M^{2+}·**3** and G **1** form extremely stable complexes in CD_2Cl_2. No mixed G-quadruplex (G **1**)$_8$·Ba^{2+}·(G **1**)$_8$·Sr^{2+}·4(**3**) was observed even 2 months after (G **1**)$_{16}$·2Ba^{2+}·4(**3**) and (G **1**)$_{16}$·2Sr^{2+}·4(**3**) were combined. A control, carried out by stirring a water solution of 1:1 Ba^{2+}·**3** and Sr^{2+}·**3** with a CD_2Cl_2 solution of G **1**, showed the expected 1:1:2 ratio of (G **1**)$_{16}$·2Ba^{2+}·4(2,6-DNP), (G **1**)$_{16}$·2Sr^{2+}·4(2,6-DNP), and mixed hexadecamer (G **1**)$_8$·Ba^{2+}·(G **1**)$_8$·

(40) For supramolecular interactions with linear Hammett correlations see: (a) Ashton, P. R.; Fyfe, M. C. T.; Hickingbottom, S. K.; Stoddart, F. J.; White, A. J. P.; Williams, D. J. *J. Chem. Soc., Perkin Trans. 2* **1998**, 2117−2128. (b) Ungaro, R.; El Haj, B.; Smid. J. *J. Am. Chem. Soc*. **1976**, *102*, 5198−5202.

(41) Since nitro groups are relatively poor hydrogen bond acceptors compared to carbonyl oxygens (Kelly, T. R.; Kim, M. H. *J. Am. Chem. Soc.* **1994**, *116*, 7072−7080), phenoxide anions with carbonyl ortho substituents should further enhance G-quadruplex kinetic stability.

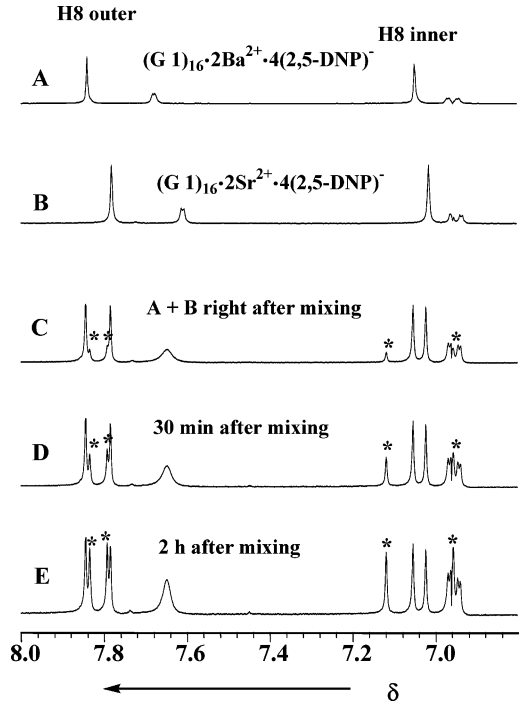

Figure 9. H8 region of the ^{1}H NMR spectra for lipophilic G-quadruplexes containing **6**: (A) (G **1**)$_{16}$·2Ba^{2+}·4(**6**); (B) (G **1**)$_{16}$·2Sr^{2+}·4(**6**); (C) a 1:1 mixture of (G **1**)$_{16}$·2Ba^{2+}·4(**6**) and (G **1**)$_{16}$·2Sr^{2+}·4(**6**) immediately after mixing; (D) 30 min after mixing; (E) 2 h after mixing. Spectra were recorded for 1.0 mM samples in CD_2Cl_2 at 25 °C. The H8 resonances for the mixed hexadecamer (G 1)$_8$·Ba^{2+}·(G **1**)$_8$·Sr^{2+}·4(**6**) are identified by asterisks. The isomerization half-life (see Figure 2) with **6** as the bound anion is $t_{1/2} = 30$ min.

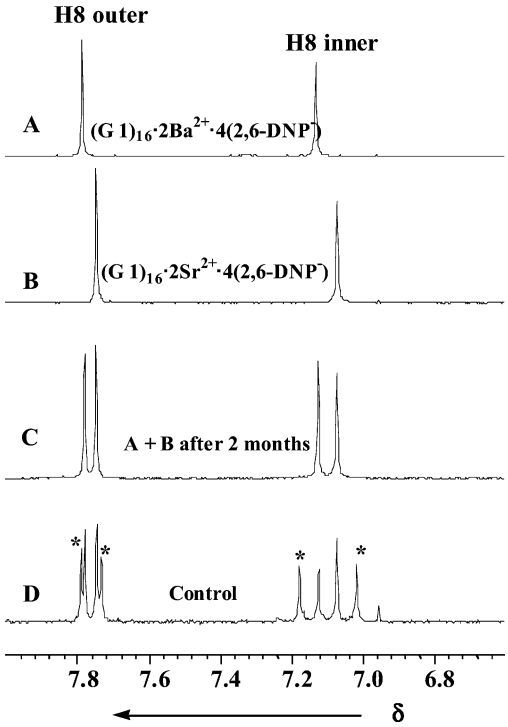

Figure 10. H8 region of the ^{1}H NMR spectra for some G-quadruplexes with **3** as the anion: (A) (G **1**)$_{16}$·2Ba^{2+}·4(**3**); (B) (G **1**)$_{16}$·2Sr^{2+}·4(**3**); (C) a 1:1 mixture of (G **1**)$_{16}$·2Ba^{2+}·4(**3**) and (G **1**)$_{16}$·2Sr^{2+}·4(**3**) 2 months after mixing; (D) a control formed by stirring a CD_2Cl_2 solution of G **1** with an aqueous solution of Ba^{2+} and Sr^{2+} phenolates for 24 h. Spectra were recorded for 1.0 mM samples in CD_2Cl_2 at 25 °C. The H8 resonances for the mixed hexadecamer (G **1**)$_8$·Ba^{2+}·(G **1**)$_8$·Sr^{2+}·4(**3**) are identified by asterisks. No isomerization of the G-quadruplexes occurred in CD_2Cl_2 with **3** as the anion.

Sr^{2+}·4(2,6-DNP). Although there are a number of possible mechanisms for formal exchange of (G **1**)$_8$·M^{2+} octamer units, the rate-determining step in this isomerization must involve displacement of the hydrogen-bonded nitrophenolate anions. The reaction is probably slow because all four of the bound **3** anions must be dissociated from the G-quadruplex before octamer exchange can occur. This just does not happen to any extent in the nonpolar CD_2Cl_2 solvent. The solvent polarity, as expected, can be used to modulate this supramolecular isomerization. Isomerization of the Ba^{2+} and Sr^{2+} complexes containing **3** as an anion was complete after 2 days in 50% CD_2Cl_2–50% CD_3CN. In this more polar solvent, G-quadruplexes with **2** (relatively stable in CD_2Cl_2 with $t_{1/2} = 42$ h) equilibrated even before an NMR spectrum could be taken (<5 min).

Conclusion

The lipophilic G-quadruplex (G **1**)$_{16}$·2Ba^{2+}·4A$^-$ is composed of four stacked G-quartets, and the inner two G-quartets are linked together by hydrogen bonding to four phenolate anions. By varying the organic anion's structure and/or basicity, we were able to control the dynamics and supramolecular isomerism of these cation-filled G-quadruplexes. This is most apparent in the anion's strong influence on rearrangement of G$_8$·M^{2+} octamers between different G-quadruplexes. The use of **3**, a relatively basic phenolate that can also form extensive hydrogen bond interactions with the two inner G$_4$-quartets, resulted in extraordinary kinetic stabilization of the G-quadruplex. No isomerization product (G **1**)$_8$·Ba^{2+}·(G **1**)$_8$·Sr^{2+}·4(**3**) was observed even 2 months after the separate G-quadruplexes (G **1**)$_{16}$·2Ba^{2+}·4(**3**) and (G **1**)$_{16}$·2Sr^{2+}·4(**3**) were combined in CD_2Cl_2. In sharp contrast, G-quadruplexes containing the isomeric **6** anion had isomerization half-lives of approximately $t_{1/2}$= 30 min under identical conditions. All the evidence indicates that the organic anion is crucial for controlling the properties of these cation-filled, lipophilic G-quadruplexes. Our studies have important implications in the use of noncovalent interactions to control the kinetic stability of hydrogen-bonded supramolecular complexes. If a self-assembled structure can be locked in place by strong noncovalent interactions with additives, then postmodification of these assemblies should be possible. One of our goals is to modify specific locations within the G-quadruplex, without having the entire complex fall apart. For example, we expect that the outer G$_4$-quartet layers will be more reactive toward ligand exchange than the inner G$_4$-quartets, because of the different interactions of these layers with bound anions. Finally, most ionophores encapsulate ions. In this system, however, anions bind to the surface of this cation-filled assembly. We are currently trying to chemically modify these anions to attach other molecules to the G-quadruplex structure.

Experimental Section

Guanosine **1** and picrate salts were prepared following published methods.[12,24] The [2.2.2]cryptand, picric acid, and phenols used to make **3**, **5**, and **6** were purchased from Aldrich. The 4-methyl-2,6-dinitrophenol used to make **4** was prepared according to the literature.[28] Other reagents and solvents were used after purification. NMR solvents were 99.0−99.9% deuterium-enriched. Proton NMR spectra were obtained with a 10 s delay to ensure accurate integration. The probe temperature was controlled to +0.1 °C. The ^{1}H NMR chemical shifts are reported in parts per million relative to the nondeuterated solvent peak.

Assignments were obtained from 2D NMR experiments. X-ray data were collected on a Bruker SMART 1000 CCD diffractometer.

Formation of [G 1]$_{16}$·2Ba^{2+}·4(Anion) Crystals. A suspension of G **1** (100 mg, 229 umol) in 5 mL of $CHCl_3$ was stirred with the appropriate salt solution in water (5 mL, 6 mM, the salt solution was generated in situ using $Ba(OH)_2$ and the corresponding phenol) at room temperature for 5 h. The organic layer was separated, the solvent was removed in vacuo, and the resulting solid was dried under vacuum. *Warning: Picric acid and picrate salts should be handled and stored with appropriate precautions!* The residue was dissolved in 1 mL of $CHCl_3$ and 4 mL of CH_3CN. This solution was evaporated slowly at room temperature in a N_2-filled desiccator to give crystals of [G **1**]$_{16}$·2Ba^{2+}·4A$^-$.

[G 1]$_{16}$·2Ba^{2+}·4(2).[12] Yellow, cubic crystals formed after 2 days, mp 258 °C dec, $[\alpha]_D = 115$ ($c = 1$ mg/mL, CH_2Cl_2). The designations a (outer G-quartet) and b (inner G-quartet) in the ^{1}H NMR data refer to the two sets of signals for the [G **1**]$_{16}$ hexadecamer: (400 MHz, CD_2Cl_2,): δ 11.31 (s, 1H, NH1$_a$), 11.09 (s, 1H, NH1$_b$), 9.61 (s, 1H, N2 H$_a$), 9.00 (s, 1H, Pic), 8.82 (s, 1H, N2 H$_b$), 7.74 (s, 1H, H8$_a$), 7.42 (s, 1H, N2 H$_b$), 7.11 (s, 1H, H8$_b$), 6.38 (s, 1H, H1′$_a$), 6.14 (d, 1H, H2′$_a$, $J = 6.0$ Hz), 5.89 (s, 1H, N2 H$_a$), 5.70 (d, 1H, H2′$_b$, $J = 4.4$ Hz), 5.59 (d, 1H, H1′$_b$, $J = 3.4$ Hz), 4.79 (d, 1H, H3′$_a$, $J = 6.0$ Hz), 4.25−4.17 (m, 4H, H4′, H5′), 4.09 (d, 1H, H3′$_b$, $J = 6.4$ Hz), 3.23−3.19 (m, 2H, H5′), 1.59 (s, 3H, CH$_{3a}$), 1.56 (s, 3H, CH$_{3b}$), 1.33 (s, 3H, CH$_{3a}$), 1.48 (s, 3H, CH$_{3b}$), 0.88 (s, 9H, Si^{t}Bu$_a$), 0.33 (s, 9H, Si^{t}Bu$_b$), 0.17 (s, 6H, SiCH$_{3a}$), −0.36 (s, 6H, SiCH$_{3b}$). ^{13}C NMR (125.7 MHz, CD_2Cl_2): δ −10.69, −6.62, −5.92, −5.83, −4.67, −4.45, −1.07, 2.82, 18.32, 18.46, 23.62, 24.69, 24.81, 25.72, 26.18, 27.07, 27.90, 31.47, 63.72, 64.73, 81.52, 82.10, 82.31, 88.04, 89.80, 91.51, 93.17, 113.09, 114.94, 115.13, 127.21, 137.54, 140.97, 142.03, 152.47, 152.92, 153.98, 159.84, 160.59, 162.36. ESI-MS: *m*/*z* 3688.47 [G **1**$_{16}$·2Ba·2Pic]$^{2+}$.

[G 1]$_{16}$·2Ba^{2+}·4(3). This complex was obtained as yellow, cubic crystals, mp 258−260 °C dec. ^{1}H NMR (400 MHz, CD_2Cl_2): δ 11.32 (s, 1H, NH1$_a$), 11.01 (s, 1H, NH1$_b$), 9.65 (s, 1H, N2 H$_{Aa}$), 8.72 (s, 1H, N2 H$_{Ab}$), 8.11 (s, 1H, N2 H$_{Bb}$), 8.10 (d, 2H, anion *m*-H, $J = 8.1$ Hz), 7.79 (s, 1H, H8$_a$), 7.13 (s, 1H, H8$_b$), 6.48 (s, 1H, H1′$_a$), 6.25 (t, 1H, anion *p*-H, $J = 8.1$ Hz), 6.17 (d, 1H, H2′$_a$, $J = 6.0$ Hz), 5.85 (s, 1H, N2 H$_{Ba}$), 5.83 (t, 1H, H2′$_b$, $J = 4.0$ Hz), 5.56 (d, 1H, H1′$_b$, $J = 3.7$ Hz), 4.80 (d, 1H, H3′$_a$, $J = 6.0$ Hz), 4.28−4.16 (m, 4H, H4′, H5′), 3.64 (d, 1H, H3′$_b$, $J = 6.4$ Hz), 3.62 (d, 1H, H5′$_b$, $J = 9.3$ Hz), 3.19−3.11 (m, 2H, H5′), 1.58 (s, 3H, CH$_{3a}$), 1.56 (s, 3H, CH$_{3b}$), 1.53 (s, 3H, CH$_{3b}$), 1.27 (s, 3H, CH$_{3a}$), 0.87 (s, 9H, Si^{t}Bu$_a$), 0.55 (s, 9H, Si^{t}Bu$_b$), 0.17 (s, 6H, SiCH$_{3a}$), 0.15 (s, 6H, SiCH$_{3b}$), −0.34 (s, 3H, SiCH$_{3b}$), −0.37 (s, 3H, SiCH$_{3a}$). ^{13}C NMR (125.7 MHz, CD_2Cl_2): δ ∠5.92, −5.84, −4.76, −4.35, 18.31, 18.48, 24.38, 24.61, 24.66, 25.75, 26.21, 27.07, 28.11, 63.72, 64.69, 81.45, 82.09, 82.43, 88.11, 89.76, 91.27, 93.43, 105.18, 112.82, 114.59, 114.89, 115.04, 132.33, 137.37, 141.30, 143.60, 152.55, 152.88, 153.06, 154.13, 159.85, 160.63, 161.03.

[G 1]$_{16}$·2Ba^{2+}·4(4). This complex was obtained as orange, cubic crystals. ^{1}H NMR (400 MHz, CD_2Cl_2): δ 11.39 (s, 1H, NH1$_a$), 10.98 (s, 1H, NH1$_b$), 9.60 (s, 1H, N2 H$_{Aa}$), 8.67 (s, 1H, N2 H$_{Ab}$), 8.14 (s, 1H, N2 H$_{Bb}$), 7.88 (s, 1H, H8$_a$), 7.79 (s, 2 H, anion H), 7.12 (s, 1H, H8$_b$), 6.47 (s, 1H, H1′$_a$), 6.15 (d, 1H, H2′$_a$, $J = 6.0$ Hz), 5.85 (s, 1H, N2 H$_{Ba}$), 5.79 (t, 1H, H2′$_b$, $J = 4.0$ Hz), 5.55 (d, 1H, H1′$_b$, $J = 3.7$ Hz), 4.78 (d, 1H, H3′$_a$, $J = 6.0$ Hz), 4.20−4.10 (m, 4H, H4′, H5′), 3.64 (d, 1H, H3′$_b$, $J = 6.4$ Hz), 3.62 (d, 1H, H5′$_b$, $J = 9.3$ Hz), 3.15 (m, 2H, H5′), 2.25 (s, 3H, anion CH$_3$) 1.58 (s, 3H, CH$_{3a}$), 1.56 (s, 3H, CH$_{3b}$), 1.53 (s, 3H, CH$_{3b}$), 1.27 (s, 3H, CH$_{3a}$), 0.84 (s, 9H, Si^{t}Bu$_a$), 0.52 (s, 9H, Si^{t}Bu$_b$), 0.15 (s, 6H, SiCH$_{3a}$), 0.13 (s, 6H, SiCH$_{3b}$), −0.39 (s, 3H, SiCH$_{3b}$), −0.41 (s, 3H, SiCH$_{3a}$).

[G 1]$_{16}$·2Ba^{2+}·4(5). This complex was obtained as red, cubic crystals. ^{1}H NMR (400 MHz, CD_2Cl_2): δ 11.34 (s, 1H, NH1$_a$), 10.98 (s, 1H, NH1$_b$), 9.59 (s, 1H, N2 H$_{Aa}$), 8.68 (s, 1H, N2 H$_{Ab}$), 8.18 (s, 1H, N2 H$_{Bb}$), 8.10 (d, 2H, m−H of anion), 7.81 (s, 2H, anion H), (7.78 (s, 1H, H8$_a$), 7.09 (s, 1H, H8$_b$), 6.48 (s, 1H, H1′$_a$) 6.17 (d, 1H, H2′$_a$, $J = 6.0$ Hz), 6.17 (s, 1H, N2 H$_{Ba}$), 5.79 (t, 1H, H2′$_b$, $J = 4.0$ Hz), 5.55 (d, 1H, H1′$_b$, $J = 3.7$ Hz), 4.77 (d, 1H, H3′$_a$, $J = 6.0$ Hz), 4.25−4.06 (m, 4H, H4′, H5′), 3.82 (s, 3H, OMe), 3.66 (d, 1H, H3′$_b$, $J = 6.4$ Hz), 3.62 (d, 1H, H5′$_b$, $J = 9.3$ Hz), 3.15 (m, 2H, H5′), 1.55 (s, 3H, CH$_{3a}$), 1.54 (s, 3H, CH$_{3b}$), 1.47 (s, 3H, CH$_{3b}$), 1.26 (s, 3H, CH$_{3a}$), 0.86 (s, 9H, Si^{t}Bu$_a$), 0.53 (s, 9H, Si^{t}Bu$_b$), 0.15 (s, 6H, SiCH$_{3a}$), 0.13 (s, 6H, SiCH$_{3b}$), −0.38 (s, 3H, SiCH$_{3b}$), −0.39 (s, 3H, SiCH$_{3a}$).

[G 1]$_{16}$·2Ba^{2+}·4(6). This complex was obtained as red, cubic crystals, mp 261−263 °C dec. ^{1}H NMR (400 MHz, CD_2Cl_2): δ 11.65 (s, 1H, NH1$_a$), 11.20 (s, 1H, NH1$_b$), 9.59 (s, 1H, N2 H$_{Aa}$), 8.83 (s, 1H, N2 H$_{Ab}$), 8.22 (br s, 1H, N2 H$_{Bb}$), 8.10 (d, 1H, *m*-H of anion, $J = 9.5$ Hz), 7.78 (s, 1H, H8$_a$), 7.68 (s, 1H, *o*-H of anion), 7.06 (s, 1H, H8$_b$), 6.95 (d, 1H, *p*-H of anion, $J = 9.5$ Hz), 6.31 (s, 1H, H1′$_a$), 6.17 (d, 1H, H2′$_a$, $J = 6.0$ Hz), 5.76 (s, 1H, N2 H$_{Ba}$), 5.70 (d, 1H, H2′$_b$, $J = 4.4$ Hz), 5.49 (d, 1H, H1′$_b$, $J = 3.4$ Hz), 4.80 (d, 1H, H3′$_a$, $J = 6.0$ Hz), 4.26−4.21 (m, 4H, H4′, H5′), 3.95 (d, 1H, H3′$_b$, $J = 6.4$ Hz), 3.60 (d, 1H, H5′$_b$, $J = 9.3$ Hz), 3.27−3.25 (d, 2H, H5′, $J = 6.0$ Hz), 1.59 (s, 3H, CH$_{3a}$), 1.58 (s, 3H, CH$_{3b}$), 1.48 (s, 3H, CH$_{3b}$), 1.26 (s, 3H, CH$_{3a}$), 0.88 (s, 9H, Si^{t}Bu$_a$), 0.56 (s, 9H, Si^{t}Bu$_b$), 0.13 (s, 6H, SiCH$_{3a}$), 0.11 (s, 6H, SiCH$_{3b}$), −0.31 (s, 3H, SiCH$_{3b}$), −0.33 (s, 3H, SiCH$_{3a}$). ^{13}C NMR (125.7 MHz, CD_2Cl_2): δ ∠5.83, −5.77, −4.87, −4.43, 18.30, 18.47, 24.38, 24.66, 25.76, 26.18, 26.98, 27.07, 27.82, 63.59, 64.56, 80.97, 81.85, 82.30, 87.43, 89.55, 91.48, 93.44, 113.07, 114.96, 115.06, 115.43, 128.50, 137.62, 141.24, 152.13, 152.45, 152.96, 154.21, 159.94, 160.66.

EXSY NMR. The 2D ^{1}H−^{1}H NMR EXSY experiments used the NOESY (Bruker XWINNMR Version 2.0) pulse sequence 90°∠t_1−90°∠t−90°∠acq. Experiments were performed on samples containing a 1 mM concentration of the G-quadruplex (which is 4 mM in anion) and a 2 mM concentration of the corresponding [2.2.2]-cryptate·BaA$_2$ salt complex at −10 °C in CD_2Cl_2. Mixing times were varied from 50 ms to 1 s, and the data used to compare the various complexes for their anion exchange rate were chosen as τ_m= 80 ms. The experiment was conducted in the phase-sensitive mode using the TPPI method with a 4 s relaxation delay. The spectral width was 8003 Hz in each dimension, and 48 scans were collected for each increment. A total of 512 files were collected, resulting in a 512 × 2048 data matrix. Line broadening of 2 Hz in the F2 dimension and 7 Hz in the F1 dimension was imposed prior to Fourier transformation. Off-diagonal peaks indicated exchange between bound and free anions. Peak intensities, I_{ij} (i, j = bound and free anion), were measured using the WINNMR program (Bruker). The relationship between the 2D peak intensities (I_{ij}) at mixing time τ_m and the exchange rate constants is given by the equation $I_{ij}(\tau_m) = (e^{-R\tau_m})_{ij} M_j^\circ$, where M_j° is the equilibrium magnetization of nuclei in site j and R has off-diagonal elements $R_{ij} = -k_{ji}$, where k_{ji} is the first-order rate constant for chemical exchange from site j to site i. The rate constants k_{ij} and k_{ji} were calculated using Perrin's matrix method.[36] Calculations were done using MathCAD 7 software (MathSoft Inc.). The mean exchange lifetime τ was calculated from the relationship to the measured first-order rate constants k_{ij} and k_{ji}, $\tau = 1/k$ (k is the average exchange rate constant, $k = (k_{ij} + k_{ji})/2$).

ESI-MS of G-Quadruplexes. A modified Bruker Daltonics (Billerica, MA) Apex II 70e actively shielded Fourier transform ion cyclotron resonance mass spectrometer was used in the positive ionization mode using a home-built micro-ESI source. The G-quadruplex solutions (~0.4 mg/mL in 20% chloroform, 80% acetonitrile) were introduced into the mass spectrometer at a flow rate of ~10 μL/h. A source potential of 3.5 kV was applied to produce a stable ion current. Ions were accumulated in an external ion reservoir comprised of an rf-only hexapole, a grounded skimmer cone, and an auxiliary electrode for 2.3 s prior to transfer into the trapped ion cell for mass analysis. Spectral acquisition was performed in the continuous duty cycle mode, whereby ions are accumulated in the hexapole ion reservoir simultaneous with ion detection in the trapped ion cell. Following a 4 ms transfer event, in which ions were transferred to the trapped ion cell, the ions were subjected to a 1.6 ms chirp excitation corresponding to *m*/*z* 8000−400. Data were acquired over an *m*/*z* range of 400−5000 (1 M data points with a sampling rate of 909 kHz). Each spectrum is the result of adding eight transients. Transients were zero-filled prior to the magnitude mode Fourier transform.

Acknowledgment. We thank the Separations and Analysis Division, Basic Energy Sciences, U.S. Department of Energy, for supporting this work. J.T.D. thanks the Dreyfus Foundation for a Teacher-Scholar Award. We thank Monique Koppel, Frank Kotch, and Dr. Yiu-fai Lam for their help with the EXSY NMR experiments.

Supporting Information Available: Crystallographic information files (CIF) including coordinates, bond lengths and angles, hydrogen bond lengths and angles, and anisotropic displacement values. This material is available free of charge via the Internet at http://pubs.acs.org.

JA035267N